AFRL-AFOSR-VA-TR-2019-0327

An advanced numerical approach for wave propagation problems in isotropic and aniso-tropic composite and
functionally graded materials. Application to high-frequency pulse propagation in the Hopkinson

Alexander Idesman
TEXAS TECH UNIVERSITY SYSTEM

09/06/2019
Final Report

Air Force Research Laboratory
AF Office Of Scientific Research (AFOSR)/ RTA2
Arlington, Virginia 22203
Air Force Materiel Command

DISTRIBUTION A: Distribution approved for public release.

REPORT DOCUMENTATION PAGE

Form Approved
OMB No. 0704-0188

1. REPORT DATE *(DD-MM-YYYY)*
11-11-2019

2. REPORT TYPE
Final Performance

3. DATES COVERED *(From - To)*
01 Aug 2016 to 31 Jul 2019

4. TITLE AND SUBTITLE
An advanced numerical approach for wave propagation problems in isotropic and aniso-tropic composite and functionally graded materials. Application to high-frequency pulse propagation in the Hopkinson

5a. CONTRACT NUMBER

5b. GRANT NUMBER
FA9550-16-1-0177

5c. PROGRAM ELEMENT NUMBER
61102F

6. AUTHOR(S)
Alexander Idesman

5d. PROJECT NUMBER

5e. TASK NUMBER

5f. WORK UNIT NUMBER

7. PERFORMING ORGANIZATION NAME(S) AND ADDRESS(ES)
TEXAS TECH UNIVERSITY SYSTEM
2500 BROADWAY
LUBBOCK, TX 79409-1105 US

8. PERFORMING ORGANIZATION REPORT NUMBER

9. SPONSORING/MONITORING AGENCY NAME(S) AND ADDRESS(ES)
AF Office of Scientific Research
875 N. Randolph St. Room 3112
Arlington, VA 22203

10. SPONSOR/MONITOR'S ACRONYM(S)
AFRL/AFOSR RTA2

11. SPONSOR/MONITOR'S REPORT NUMBER(S)
AFRL-AFOSR-VA-TR-2019-0327

12. DISTRIBUTION/AVAILABILITY STATEMENT
A DISTRIBUTION UNLIMITED: PB Public Release

13. SUPPLEMENTARY NOTES

14. ABSTRACT
A new high-order accurate numerical approach has been developed for wave propagation in isotropic and anisotropic composite and functionally graded materials. It does not use any weak formulation for the derivation of the semi-discrete system of equations. The coefficients of the semi-discrete system of equations are directly derived from the minimization of the order of the local truncation error and provide the optimal order of accuracy. The new approach is much more accurate than other known numerical techniques (e.g., finite elements, isogeometric elements, finite volume method and other) . A new highorder accurate procedure has been also developed for the Dirichlet and Neumann boundary conditions that includes the time and spatial derivatives of the boundary conditions. This provides the same high order of accuracy of the stencils for internal and boundary points. The new approach has been first tested on rectangular domains and has shown a significant decrease in the computation time (by a factor of 10 - 1000 and more) compared to that for the high-order isogeometric elements at the same accuracy. The application of the new high-order accurate approach to complicated irregular domains shows a much bigger decrease in the computational costs.

15. SUBJECT TERMS
elastodynamics, filtering, finite element

16. SECURITY CLASSIFICATION OF:			17. LIMITATION OF ABSTRACT	18. NUMBER OF PAGES	19a. NAME OF RESPONSIBLE PERSON
a. REPORT	b. ABSTRACT	c. THIS PAGE			FAHROO, FARIBA
Unclassified	Unclassified	Unclassified	UU		

					19b. TELEPHONE NUMBER *(Include area code)* 703-696-8429

An Advanced Numerical Approach for Wave Propagation Problems in Isotropic and Anisotropic Composite and Functionally Graded Materials

Alexander Idesman
Texas Tech University

Final report

The main accomplishments with the technical details have been reported in the archival publications. Therefore, below we will list the main findings with the corresponding figures from our presentations at the 2017-2019 Program Review Meetings and short explanations. We also include the references to our publications for the detailed derivations and explanations.

Main accomplishments

1. A new high-order numerical approach for the wave (heat) propagation on regular domains

A prohibitively large computation time for the simulation of real-world wave propagation problems is one of the issues of existing numerical techniques. We planned to resolve this issue by the reduction of the numerical dispersion error of numerical techniques that should lead to a significant increase in accuracy and the reduction in the computational costs. However, working on the project we have developed a more general numerical approach that provides an optimal accuracy of the discrete equations not only for the wave equations but also for other partial differential equations. This approach is based on the minimization of the local truncation error and at the same computational costs it significantly exceeds the accuracy of known numerical techniques for wave propagation. We call the new approach as the optimal local truncation error method (OLTEM). In this section we shortly discuss the derivation of OLTEM for the time dependent wave and heat equations.
As a mesh, the internal grid points of a uniform Cartesian rectangular (square) mesh that are located inside the domain as well as the points at the intersection of the boundary of a complex irregular domain with the horizontal, vertical and diagonal grid lines of the uniform Cartesian mesh are used with the new approach; i.e., in contrast to the finite element meshes, a trivial mesh is used with the new approach. The idea of the OLTEM is very simple. We start the development of a new numerical technique by assuming a compact stencil equation for each internal grid point (there are no stencils for the boundary points; the boundary points contribute to the stencils of the internal points). A stencil equation is a linear combination of the values of the numerical solution of the function (for a discrete system) or the function and its time derivatives (for a semidiscrete system) at a number of neighboring grid points where the coefficients of the stencil equations are assumed to be unknown. These unknown coefficients are determined by the minimization of the order of the local truncation error for each stencil equation. This procedure includes a Taylor series expansion of the unknown exact solution at the grid points and its substitution into the stencil equation. As a result, we obtain the local truncation error in the form of a Taylor series. At this point, no information about partial differential equations is used. Then, the corresponding

partial differential equations are considered at the grid points in order to exclude some partial derivatives in the expression for the local truncation error (for the wave equation we replace all time derivatives by the spatial derivatives). Finally, the unknown coefficients of the stencil equation are calculated from a small local system of algebraic equations obtained by equating to zero the lowest terms in the Taylor series expansion of the local truncation error. The coefficients of the stencil equations are similarly calculated for the uniform and nonuniform stencils for grid points located far and close to the boundary. Then, the stencils for all internal grid points form a fully discrete or semidiscrete global system of equations that can be easily solved. The implementation of this idea for the wave (heat) equation is shortly presented in Figs. 1-3 with simple 9-point stencils (see our papers [1-6,8-12] for the detailed derivations as well as more complicated stencils).

Wave and Heat Equations with 9-point Stencils on Uniform Meshes [1,2]

Spatial location of the degrees of freedom u_i (with $h = dx$)

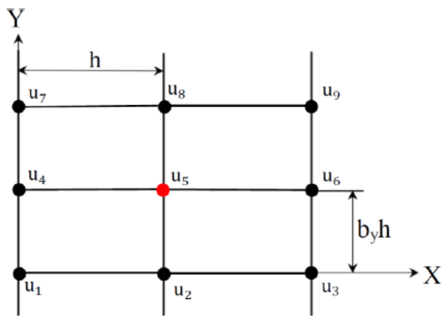

$$M\ddot{U} + KU = R$$

9-point stencil equation (similar to linear FEs):

$$\sum_{i=1}^{9} h^2 m_i \frac{d^n u_i^{num}}{dt^n} + \sum_{i=1}^{9} k_i\, u_i^{num} = 0 \qquad (1)$$

Coefficients m_i and k_i $(i = 1,2, \dots, 9)$ to be determined

Local truncation error:

$$e = \sum_{i=1}^{9} h^2 m_i \frac{d^n u_i}{dt^n} + \sum_{i=1}^{9} k_i\, u_i \qquad (2)$$

u_i corresponds to the exact solution at the grid points i $(i=1,2,\dots,9)$

$$e = \sum_{i=1}^{9} h^2 m_i \left(\frac{d^n u_i}{dt^n} - \frac{d^n u_i^{num}}{dt^n}\right) + \sum_{i=1}^{9} k_i \left(u_i - u_i^{num}\right) \qquad (3)$$

[1] A. Idesman, B. Dey, The use of the local truncation error for the increase in accuracy of the linear finite elements for heat transfer problems, Comput. Methods Appl. Mech. Engrg., 319, 2017, pp. 52-82.
[2] A. Idesman, The use of the local truncation error to improve arbitrary-order finite elements for the linear wave and heat equations., Comput. Methods Appl. Mech. Engrg., 334, 2018, pp. 268-312.

Fig. 1. The derivation of the new approach for the time dependent wave (heat) equation on uniform meshes

The main advantages of the new approach are a high optimal accuracy and the simplicity of the formation of a discrete (semi-discrete) system of equations for irregular domains. Changing the width of the stencil equations, different linear and high-order numerical techniques can be developed. We should mention that the new approach also improves the accuracy of the numerical results for uniform stencils on regular domains compared to that of existing techniques. For example, it has been shown that at the same width of the stencils (at the same computational costs) as those for the linear finite elements and for the high-order isogeometric elements, the new approach increases the accuracy from order 2p (the linear finite elements and the high-order isogeometric elements) to order 4p (the new approach) for the wave and heat equations on regular rectangular domains where p≥1 is the order of the corresponding elements. This leads to a huge reduction in the computation time at a given accuracy.

Wave and Heat Equations with 9-point Stencils on Uniform Meshes [1,2]

Equations for the exact solution:

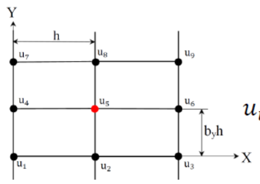

Taylor series:

$$u_i = u_5 + \frac{\partial u_5}{\partial x}(\pm ih) + \frac{\partial u_5}{\partial y}(\pm jb_y h) + \frac{\partial^2 u_5}{\partial x^2}\frac{(\pm ih)^2}{2!} + \frac{\partial^2 u_5}{\partial x \partial y}\frac{(\pm ih)(\pm jb_y h)}{2!} + \frac{\partial^2 u_5}{\partial y^2}\frac{(\pm jb_y h)^2}{2!} + \cdots \quad (1)$$

$$\frac{\partial^n u_i}{\partial t^n} = \frac{\partial^n u_5}{\partial t^n} + \frac{\partial^{n+1} u_5}{\partial t^n \partial x}[(l-2)h] + \frac{\partial^{n+1} u_5}{\partial t^n \partial y}[(j-2)b_y h] + \frac{\partial^{n+2} u_5}{\partial t^n \partial x^2}\frac{[(l-2)h]^2}{2!} + \frac{\partial^{n+2} u_5}{\partial t^n \partial x \partial y}\frac{[(l-2)h][(j-2)b_y h]}{2!} + \frac{\partial^{n+2} u_5}{\partial t^n \partial y^2}\frac{[(j-2)b_y h]^2}{2!} + \cdots \quad (2)$$

with $i=3(j-1)+l$, *and* $l,j=1,2,3,\ldots$

PDE:

$$\frac{d^n u_5}{dt^n} = \bar{c}\nabla^2 u_5 \quad (3) \qquad \frac{\partial^{(2p+2k+n)} u_5}{\partial x^{2p}\partial y^{2k}\partial t^n} = \bar{c}\frac{\partial^{(2p+2k)}\nabla^2 u_5}{\partial x^{2p}\partial y^{2k}}, \quad (4)$$

with $p=0,1,2,3,\ldots$ *and* $k=1,2,3,\ldots$

LTE:

$$e = \sum_{i=1}^{9} h^2 m_i \frac{d^n u_i}{dt^n} + \sum_{i=1}^{9} k_i u_i \quad (5)$$

Inserting (1)-(4) into (5) we will get LTE as follows (see the next slide) :

Fig. 2. The derivation of the new approach for the time dependent wave (heat) equation on uniform meshes (continuation).

The Local Truncation Error

$$e = \bar{c}[\,b_1 u_5 + h^2 b_2\left(\frac{\partial^2 u_5}{\partial x^2} + \frac{\partial^2 u_5}{\partial y^2}\right) + \frac{h^4}{12}\left\{b_3\left(\frac{\partial^4 u_5}{\partial x^4} + \frac{\partial^4 u_5}{\partial y^4}\right) + b_4\frac{\partial^4 u_5}{\partial x^2 \partial y^2}\right\} + \frac{h^6}{360}\left\{b_5\left(\frac{\partial^6 u_5}{\partial x^6} + \frac{\partial^6 u_5}{\partial y^6}\right) + b_6\left(\frac{\partial^4 u_5}{\partial x^4 \partial y^2} + \frac{\partial^4 u_5}{\partial x^2 \partial y^4}\right)\right\}] + O(h^8)$$

with

$b_1 = k_1 + 4(k_2 + k_3)$, $b_2 = 2k_2 + k_3 + 4(m_2 + m_3)$,
$b_3 = 2k_2 + k_3 + 3(2m_2 + m_3)$, $b_4 = 12(2k_2 + 12(2m_2 + m_3))$,
$b_5 = 2k_2 + k_3 + 30(2m_2 + m_3)$, $b_6 = 30(k_2 + 14m_2 + m_3)$.

Local system of four equations for m_i and k_i $(i = 1, 2, 3)$

$$b_1 = 0, \quad b_2 = 0, \quad b_3 = 0, \quad b_4 = 0.$$

Solution of the local system in terms of two arbitrary coefficients a_1 and a_2

$$m_1 = a_1, \quad m_2 = a_1/4 - a_2/20, \quad m_3 = a_1/2 - a_2/8, \quad k_1 = a_2, \quad k_2 = -a_2/20, \quad k_3 = -a_2/5.$$

The local truncation error for the new approach:

$$e = \frac{\bar{c}h^6}{2400}\left[3a_2\left(\frac{\partial^6 u_5}{\partial x^6} + \frac{\partial^6 u_5}{\partial y^6}\right) + 25(24a_1 - 5a_2)\left(\frac{\partial^4 u_5}{\partial x^4 \partial y^2} + \frac{\partial^4 u_5}{\partial x^2 \partial y^4}\right)\right] + O(h^8).$$

The local truncation error for the conventional linear elements:

$$e_{FE}^{lin} = \frac{\bar{c}h^4}{12}\left(\frac{\partial^4 u_5}{\partial x^4} + \frac{\partial^4 u_5}{\partial y^4}\right) + O(h^6).$$

At similar 9-point stencils, the new approach improves the accuracy by two orders

Fig. 3. The derivation of the new approach for the time dependent wave (heat) equation on uniform meshes (continuation).

2. A new high-order numerical approach for the time independent Poisson equation on regular domains

As we mentioned in the previous section, the new approach can be equally applied to other PDEs. Here we shortly show its application with the 9-point stencils to the 2-D Poisson equation. The coefficients k_i of the stencil equations (see Fig. 4) are calculated by the minimization of the order of the local truncation error. The main difference in the derivations for the wave and Poisson equation consists in the fact that the time-independent Poisson equation is used for the exclusion of the second and higher order x-derivatives (see Fig. 4) in the expression for the local truncation error (see Fig. 5). It was shown that the maximum increase in accuracy by four orders for the 2-D and 3-D Poisson equation can be reached by the new technique with the 2-D square and 3-D cubic finite elements. The use of 2-D and 3-D rectangular Cartesian meshes decreases the accuracy of the new technique by two orders (however, it still exceeds the accuracy of the conventional linear finite elements by two orders). This means that a uniform refinement of 2-D square and 3-D cubical elements in one direction or 3-D cubical elements in two directions (i.e., transforming square (cubical) elements into smaller rectangular (brick) elements) leads to the decrease in the order of accuracy of the new technique and this should be taken into account at the selection of a refinement strategy. The detailed derivations of the new approach with simple 9-point and more complicated stencils for the Poisson equation can be found in our papers [1,2,6,910,11,12].

Poisson Equation with 9-point stencils on uniform meshes [1]

Spatial location of the degrees of freedom u_i (with h =dx)

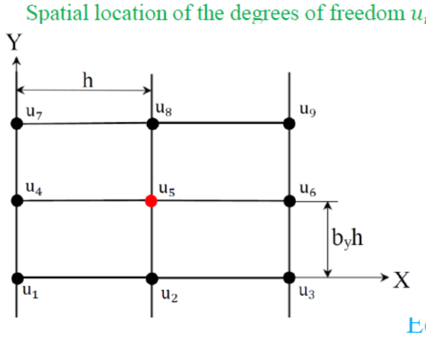

$$\boldsymbol{KU} = \boldsymbol{R}$$

Stencil equation (similar to linear FEs):

$$\sum_{i=1}^{9} k_i\, u_i^{num} = 0 \qquad (1)$$

Coefficients k_i $(i = 1,2,\ldots,9)$ to be determined

Equations for the exact solution:

Taylor series:

$$u_i = u_5 + \frac{\partial u_5}{\partial x}(\pm ih) + \frac{\partial u_5}{\partial y}(\pm j b_y h) + \frac{\partial^2 u_5}{\partial x^2}\frac{(\pm ih)^2}{2!} + \frac{\partial^2 u_5}{\partial x \partial y}\frac{(\pm ih)(\pm j b_y h)}{2!} + \frac{\partial^2 u_5}{\partial y^2}\frac{(\pm j b_y h)^2}{2!} + \cdots \qquad (2)$$

with $i=3(j-1)+l$, and $l,j=1, 2, 3, \ldots$

PDE:

$$\frac{\partial^2 u_5}{\partial x^2} = -\frac{\partial^2 u_5}{\partial y^2}, \qquad \frac{\partial^{(p+2k)} u_5}{\partial y^p \partial x^{2k}} = (-1)^j \frac{\partial^{p+2k} u_5}{\partial y^{p+2k}}, \qquad \frac{\partial^{(p+2k-1)} u_5}{\partial y^p \partial x^{2k-1}} = (-1)^j \frac{\partial^{p+2k-1} u_5}{\partial y^{p+2k-1} \partial x}$$

with $p=0, 1, 2, 3, \ldots$ and $k=1, 2, 3,$

[1] A. Idesman, B. Dey, The use of the local truncation error for the increase in accuracy of the linear finite elements for heat transfer problems, Comput. Methods Appl. Mech. Engrg., 319, 2017, pp. 52-82.

Fig. 4. The derivation of the new approach for the time-independent Poisson equation on uniform meshes

The Local Truncation error

$$e = b_1 u_5 + h^2 b_2 \frac{\partial^2 u_5}{\partial y^2} + \frac{h^4}{12} b_3 \frac{\partial^4 u_5}{\partial y^4} + \frac{h^6}{360} b_4 \frac{\partial^6 u_5}{\partial y^6} + \frac{h^8}{20160} b_5 \frac{\partial^8 u_5}{\partial y^8} + O(h^{10})$$

with

$$b_1 = k_1 + 2(2k_2 + k_3 + k_4), \qquad b_2 = 2(b_y^2 - 1)k_2 + b_y^2 k_3 - k_4,$$

$$b_3 = 2(1 - 6b_y^2 + b_y^4)k_2 + b_y^4 k_3 - k_4, \qquad b_4 = 2(-1 + 15b_y^2 - 15b_y^4 + b_y^6)k_2 + b_y^6 k_3 - k_4,$$

$$b_5 = 2(1 - 28b_y^2 + 70b_y^4 - 28b_y^6 + b_y^8)k_2 + b_y^8 k_3 + k_4.$$

Local system of equations for $k_i (i = 1, 2, 3, 4)$

$$b_1 = k_1 + 2(2k_2 + k_3 + k_4) = 0,$$
$$b_2 = 2(b_y^2 - 1)k_2 + b_y^2 k_3 - k_4 = 0,$$
$$b_3 = 2(1 - 6b_y^2 + b_y^4)k_2 + b_y^4 k_3 - k_4 = 0.$$

The local truncation error for the new approach:

$$e = \frac{a_1 b_y^2 (b_y^2 - 1) h^6}{400} \frac{\partial^6 u_5}{\partial y^6} + \frac{a_1 b_y^2 (11 - 32 b_y^2 + 11 b_y^4) h^8}{100800} \frac{\partial^8 u_5}{\partial y^8} + O(h^{10}).$$

The local truncation error for the conventional linear elements:

$$e_{FE}^{lin} = \frac{b_y (1 + b_y^2) h^4}{12} \frac{\partial^4 u_5}{\partial y^4} + \frac{b_y (b_y^2 - 1) h^6}{90} \frac{\partial^6 u_5}{\partial y^6} + \frac{b_y (1 + b_y^2)(25 - 67 b_y^2 + 25 b_y^4) h^8}{60480} \frac{\partial^8 u_5}{\partial y^8} + O(h^{10}).$$

At similar 9-point stencils, the new approach improves the accuracy by two (rectangular meshes) and four (square meshes) orders

Fig. 5. The derivation of the new approach for the time-independent Poisson equation on uniform meshes (continuation).

3. Numerical high-order boundary conditions

The new approach with the compact stencils corresponding to the quadrilateral high-order finite and isogeometric elements provides a very high order of accuracy for the internal nodes with the regular stencils (much higher than that for the quadrilateral high-order finite and isogeometric elements). However, the stencils (the cut stencils) for the degrees of freedom that are located close to the boundary include less grid points than the regular stencils and cannot provide the order of accuracy of the regular stencils. This would decrease the order of accuracy of numerical solutions for the entire domain. To resolve this issue for the new approach with the very high order of accuracy, we have developed new numerical high-order boundary conditions for the cut stencils that provide the order of accuracy of the entire numerical solution consistent with the order of accuracy of the regular stencils of the new technique. The derivation of the new high-order boundary conditions is based on the minimization of the order of the local truncation error for the cut stencils and includes the original partial differential equation and the actual boundary conditions. In addition to the regular form of the boundary conditions, the new approach includes the tangential derivatives of the boundary conditions at the boundary points; see Fig. 6. For example, the cut boundary stencil with 3 × 3 = 9 degrees of freedom for the new technique in the 2-D case provides the order of accuracy consistent with that for the regular stencil with 5 × 5 =

25 degrees of freedom. Our approach for the high-order boundary conditions is different from some known approaches for the numerical high-order boundary conditions based on the introduction of the ghost nodes and the polynomial approximations of the unknown function or the use of the inverse Lax–Wendroff procedure for the ghost nodes. We do not introduce the ghost nodes in our approach. The detailed derivations of the new numerical high-order boundary conditions can be found in our paper [3].

New high-order boundary conditions with 25-point stencils on uniform meshes in the 2-D case [1]

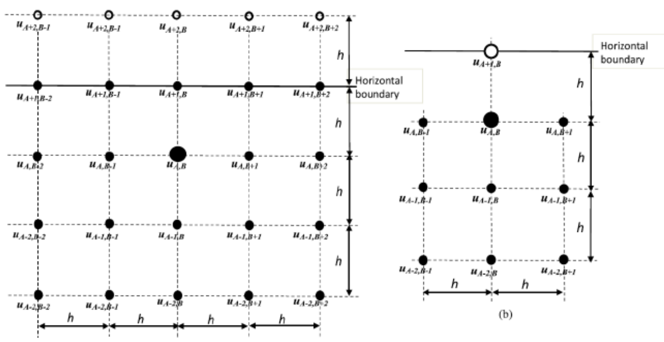

9-point cut stencil for Dirichlet boundary conditions $u_{A+1,B}=g_2(x_B,t)$ provides the 8[th] order of accuracy

$$h^2\{m_1[\frac{d^n u^{num}_{(A-2),(B-1)}}{dt^n} + \frac{d^n u^{num}_{(A-2),(B+1)}}{dt^n}] + m_2\frac{d^n u^{num}_{(A-2),B}}{dt^n} + m_3[\frac{d^n u^{num}_{(A-1),(B-1)}}{dt^n} + \frac{d^n u^{num}_{(A-1),(B+1)}}{dt^n}]$$
$$+ m_4\frac{d^n u^{num}_{(A-1),B}}{dt^n}$$
$$+ m_5[\frac{d^n u^{num}_{A,(B-1)}}{dt^n} + \frac{d^n u^{num}_{A,(B+1)}}{dt^n}] + m_6\frac{d^n u^{num}_{A,B}}{dt^n}\}$$
$$+ \bar{c}\{k_1[u^{num}_{(A-2),(B-1)} + u^{num}_{(A-2),(B+1)}] + k_2 u^{num}_{(A-2),B} + k_3[u^{num}_{(A-1),(B-1)} + u^{num}_{(A-1),(B+1)}] + k_4 u^{num}_{(A-1),B}$$
$$+ k_5[u^{num}_{A,(B-1)} + u^{num}_{A,(B+1)}] + k_6 u^{num}_{A,B}\} = f_{A,B} = \frac{a_1}{239400\bar{c}^3}(362880\bar{c}^4 g_2(x_B,t) + h^2(-30240\bar{c}^3\frac{\partial^n g_2(x_B,t)}{\partial t^n} + 756\bar{c}h^4\frac{\partial^{3n} g_2(x_B,t)}{\partial t^{3n}}$$
$$- 723h^6\frac{\partial^{4n} g_2(x_B,t)}{\partial t^{4n}}$$
$$+ 60480\bar{c}^4\frac{\partial^2 g_2(x_B,t)}{\partial x^2} - 2520\bar{c}^3h^2\frac{\partial^{2+n} g_2(x_B,t)}{\partial x^2\partial t^n} - 2268\bar{c}^2h^4\frac{\partial^{2+2n} g_2(x_B,t)}{\partial x^2\partial t^{2n}}$$
$$+ 2955\bar{c}h^6\frac{\partial^{2+3n} g_2(x_B,t)}{\partial x^2\partial t^{3n}} + 5040\bar{c}^4h^2\frac{\partial^4 g_2(x_B,t)}{\partial x^4} + 2058\bar{c}^3h^4\frac{\partial^{4+n} g_2(x_B,t)}{\partial x^4\partial t^n}$$
$$- 4527\bar{c}^2h^6\frac{\partial^{4+2n} g_2(x_B,t)}{\partial x^4\partial t^{2n}} + 168\bar{c}^4h^4\frac{\partial^6 g_2(x_B,t)}{\partial x^6} + 2381\bar{c}^3h^6\frac{\partial^{6+n} g_2(x_B,t)}{\partial x^6\partial t^n}$$
$$- 57\bar{c}^4h^6\frac{\partial^8 g_2(x_B,t)}{\partial x^8})),$$

[1] A. Idesman, The use of the local truncation error to improve arbitrary-order finite elements for the linear wave and heat equations., Comput. Methods Appl. Mech. Engrg., 334, 2018, pp. 268-312.

Fig. 6. New numerical high-order boundary conditions used by the new approach with 25-point stencils for the wave equation.

4. The comparison of accuracy of the new numerical approach with the linear finite elements and the high-order isogeometric elements at similar stencils on regular domains

Here we compare the accuracy of the new approach with the linear finite elements as well as the high-order isogeometric elements on regular domains, see Fig. 7. Compared to the linear finite elements used for the wave (heat) equation, the new approach increases the accuracy from the second order to the fourth order at the same computational costs. Compared to the linear finite elements used for the Poisson equation, the new approach increases the accuracy from the second order to the sixth order for 2-D square and 3-D cubic meshes and from the second order to the fourth order for 2-D and 3-D rectangular meshes at the same computational costs. Compared to the p-order isogeometric elements ($p \geq 2$) used for the wave (heat) equation, the new approach increases the accuracy from order 2p to order 4p at the same computational costs. Compared to the quadratic isogeometric elements used for the Poisson equation, the new approach increases the accuracy from the 6th order to the 18th order for 2-D square meshes and from the 4th order to the 14th order for 2-D rectangular meshes at the same computational costs. This huge increase in the order in accuracy of the new technique is optimal. The new approach yields the maximum possible order of accuracy among all numerical techniques with the same widths of stencil equations independent of the method used for the derivation of discrete or semidiscrete equations. This optimal order of accuracy cannot be improved without changing the widths of stencil equations; see also our papers [1-12] for more details.

Improvement of order of accuracy by reduction of order of local truncation error of stencil equation [1,2]

		Order of accuracy in space	
Governing Equation	Element type / **stencil width**	Conventional FE and ISE	New approach with similar stencils [1, 2]
Time dependent wave equation and heat equations	Linear finite elements (p=1, 2-D 9-point stencils)	**2 (2p)**	**4 (4p)**
	Quadratic isogeometric elements (p=2, 2-D 25-point stencils)	**4 (2p)**	**8 (4p)**
Poisson Equation	Linear finite elements (p=1, 2-D 9-point stencils)	**2**	**4** (rectangular meshes) **6** (square meshes)
	Quadratic isogeometric elements (p=2, 2-D 25-point stencils)	**4** (rectangular meshes) **6** (square meshes)	**14** (rectangular meshes) **18** (square meshes)

- The new approach with a huge increase in the order of accuracy to 4p requires the same computational costs as those of the conventional finite and isogeometric elements with the order of accuracy of 2p.
- The new approach yields the maximum possible order of accuracy for the selected structure of the stencil equation that cannot be exceeded without changing the number of points in the stencil equation.

[1] A. Idesman, B. Dey, The use of the local truncation error for the increase in accuracy of the linear finite elements for heat transfer problems, Comput. Methods Appl. Mech. Engrg., 319, 2017, pp. 52-82.

[2] A. Idesman, The use of the local truncation error to improve arbitrary-order finite elements for the linear wave and heat equations., Comput. Methods Appl. Mech. Engrg., 334, 2018, pp. 268-312.

Fig. 7. The comparison of accuracy of the new numerical approach with the linear finite elements and the p-order isogeometric elements ($p \geq 2$) at similar stencils on regular domains.

5. The development of the new numerical approach for irregular domains

We have developed the new approach with the 2-D 9-point stencils and the 3-D 27-point stencils (similar to the stencils for the linear finite elements) for the wave, heat and Poisson equations on irregular domains using trivial Cartesian meshes. The new approach provides the same order of accuracy on regular (see the previous sections) and irregular domains and significantly exceeds the accuracy of the linear and high-order finite elements (see the numerical examples below).
The 9-point uniform stencils in the 2-D case are similar to those for the 2-D linear quadrilateral finite elements. The spatial locations of the 8 degrees of freedom that are close to the internal degree of freedom u_5 and contribute to the 9-point uniform stencil for this degree of freedom are shown in Fig. 8 for the case when the boundary and the Cartesian mesh are matched or when the degree of freedom u_5 is located far from the boundary. In the case of non-matching grids when the grid points do not coincide with the boundary, the first grid points that lie outside the physical domain are moved to the boundary of the physical domain; see Fig. 8 for the nonuniform stencil. In order to find the boundary points that are included into the nonuniform stencil for the degree of freedom u_5 (see Fig. 8) we join the central point u_5 with the 8 closest grid points; i.e., we have eight straight lines along the x- and y-axes and along the diagonal directions (the dashed lines) of the grid; see Fig. 8. If any of these lines intersects the boundary of the domain then the corresponding grid point (designated as ○) should be moved to the boundary (the new location is designated as ●). This means that for all internal points located within the domain we use 9-point uniform or non-uniform stencils (see Fig. 8). Similar trivial procedure is used in order to form the 27-point uniform and non-uniform stencils in the 3-D case; see Fig. 9. The stencil coefficients for the non-uniform stencils are calculated by the minimization of the order of the local truncation error (similar to those for the uniform stencils in the previous sections); see the summary of the new approach on irregular domains in Fig. 10 and our papers [1,2,10,11,12] for the detailed derivations and explanations.

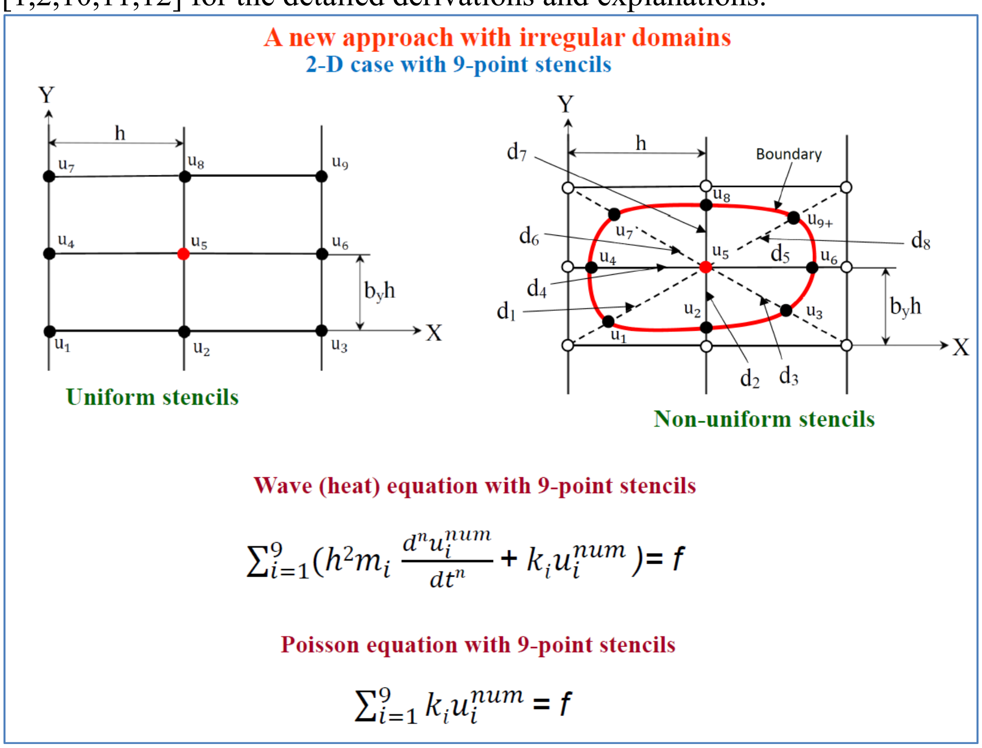

Fig.8. The 9-point uniform and non-uniform stencils used with the new approach in the 2-D case.

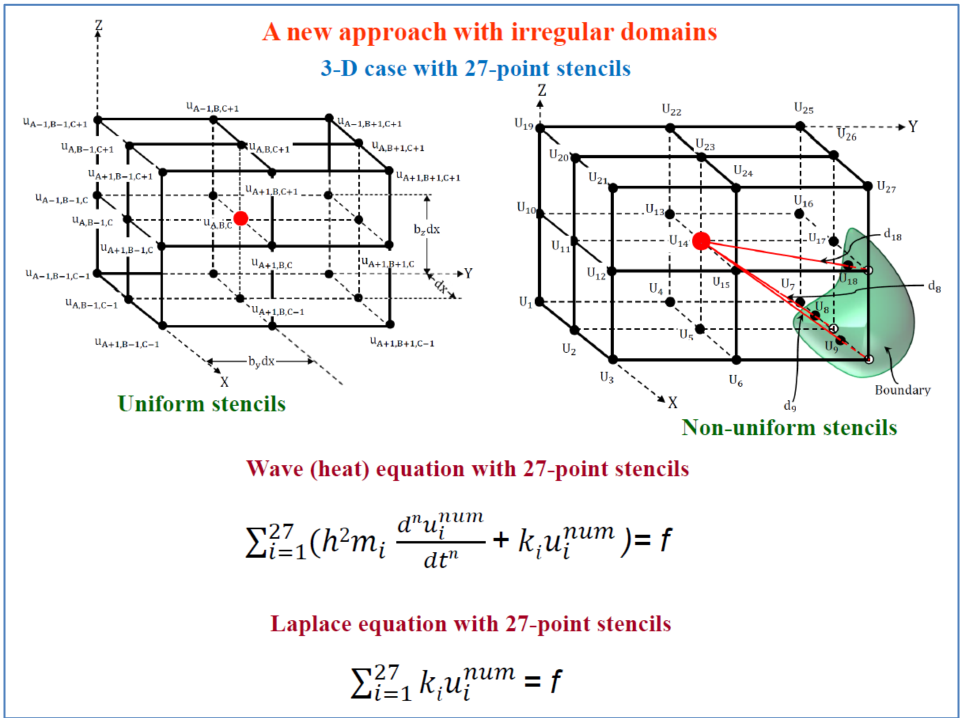

Fig.9. The 27-point uniform and non-uniform stencils used with the new approach in the 3-D case.

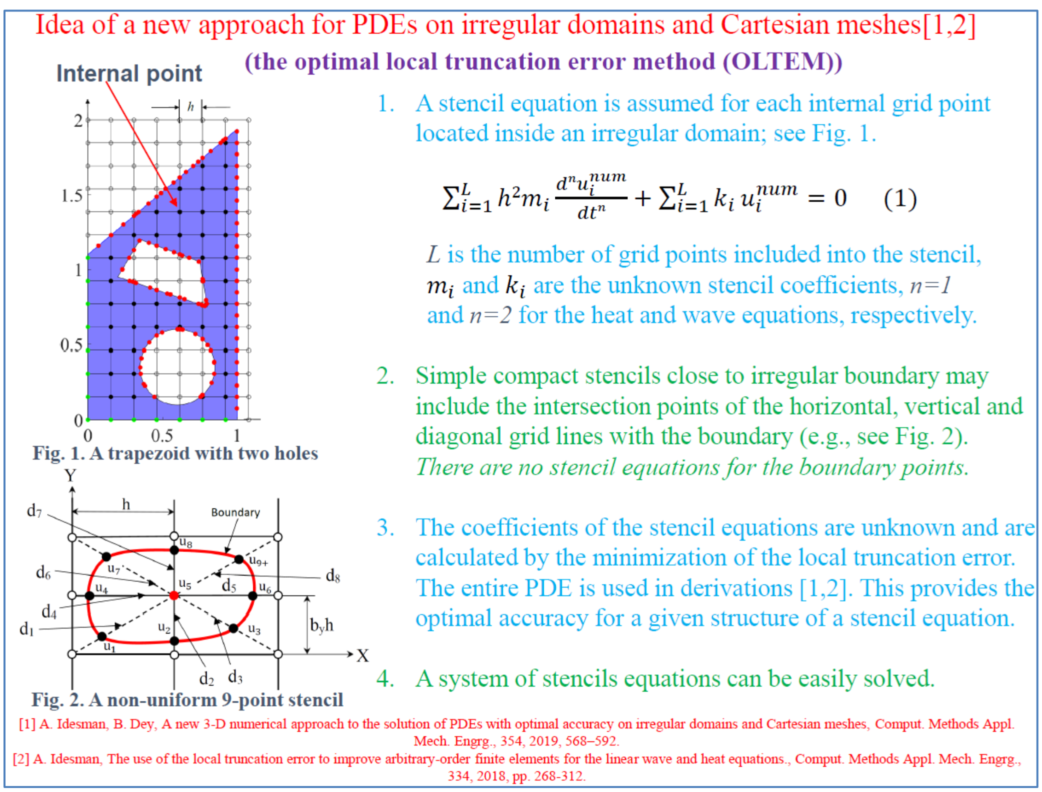

Fig.10. The summary of the new approach for the solution of PDEs on irregular domains with Cartesian meshes.

6. Solution of benchmark problems and comparison with the known numerical techniques

For the problems considered in this and following sections we use the method of manufactured solutions for which the exact solutions of the problem are known and the exact numerical error can be easily calculated. Below we study the convergence rate for the new approach with the 2-D 25-point stencils that is applied to the solution of the wave equation on a regular square domain; see Fig. 11 for the exact solution and the numerical results (curve 2). For comparison, the solution of the same problem by the quadratic isogeometric elements with similar 25-point stencils is presented by curve 1. As can be seen, at similar 25-point stencils, the accuracy of the new approach exceeds the accuracy of the quadratic isogeometrc elements by four orders. This is in agreement with the theoretical results of section 1. The detailed description of this benchmark problem as well as that for the Poisson equation on regular domains can be found in our papers [9].

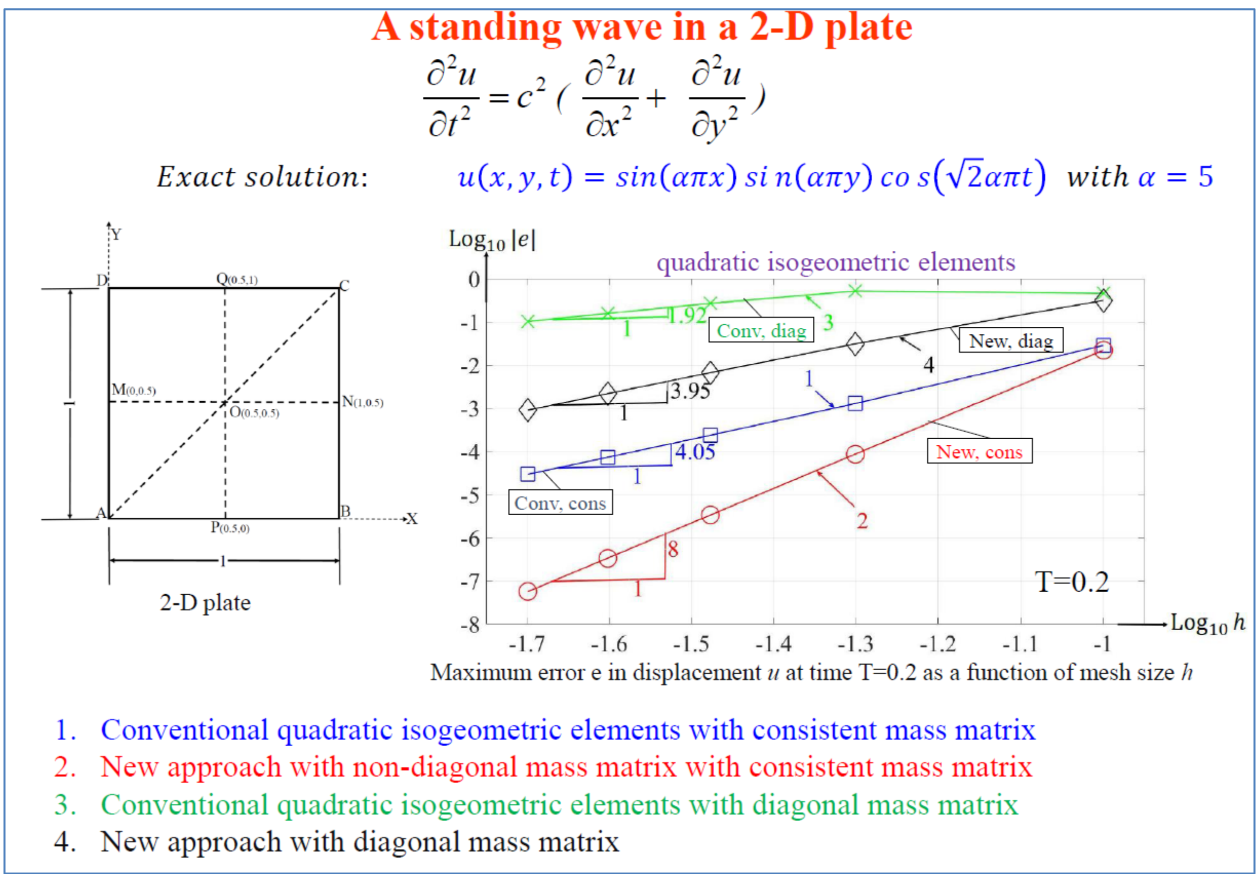

Fig. 11. The convergence rate of the new approach with the 2-D 25-point stencils that is applied to the solution of the wave equation on a regular square domain; see curve 2. Curve 1 corresponds to the solution obtained by the quadratic isogeometric elements with similar 25-point stencils.

7. The application of the new approach to wave propagation problems on complex irregular domains

7.1. 2-D highly oscillatory waves on a complex irregular domain with two holes.

Let us consider a trapezoidal plate OPQR with a quadrilateral hole ABCD and a 4-sector hole; see Fig. 12. Using the method of manufactured solutions, we select a highly oscillatory exact solution; see Fig. 12. This solution has many local minima and maxima for the displacement and for the velocity on the considered irregular domain; see Fig. 12. The problem was solved by the new approach (9-point stencils) with 11263, 15609 and 48210 degrees of freedom and by the conventional linear triangular finite elements with 652462 and 1277691 degrees of freedom (typical meshes used by the new approach and by FEM are shown in Fig. 13). The computation time on the desktop computer (Intel(R) Core(TM) i7-4790 CPU @ 3.60GHz with 16.0 GB RAM) was about 17 minutes for the new approach with 48210 degrees of freedom (using our non-optimized Matlab code) and about 11 hours for the linear finite elements with 652462 degrees of freedom using the modern commercial code COMSOL on the same desktop computer. Fig. 14 shows the distribution of the relative errors in velocity and in displacement of the numerical solutions for these two techniques. As can be seen from Fig. 14, the maximum error for the numerical results obtained by the new approach is close to 1.5% for both displacements and velocities. With the second order linear finite elements we can predict that for the maximum error of 1.5% (the same as for the new approach) we need to increase the number of degrees of freedom to approximately 13 000 000; i.e., at the 1.5% accuracy the new approach reduces the number of degrees of freedom by a factor of 270 (see the table in Fig. 14). In this case, we were not able to solve this problem by the linear finite elements on our desktop computer due to a prohibitively large computational time. Moreover, in contrast to the complicated mesh generators used by the finite elements, the new approach uses trivial Cartesian meshes for complex irregular domains; see our paper [11] for more details.

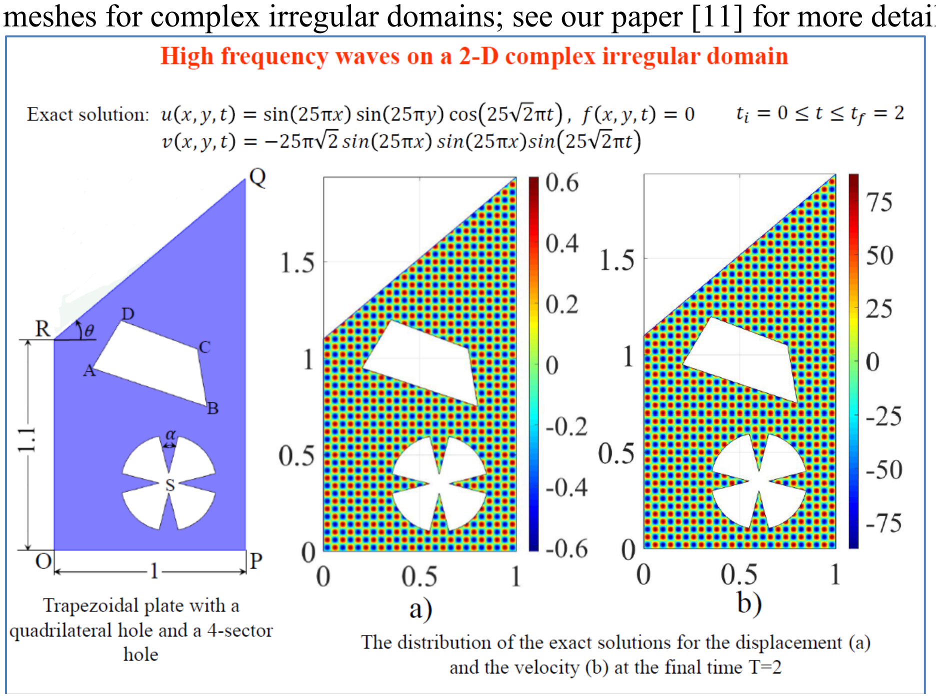

Fig.12. Highly oscillatory waves in a trapezoidal plate with two holes.

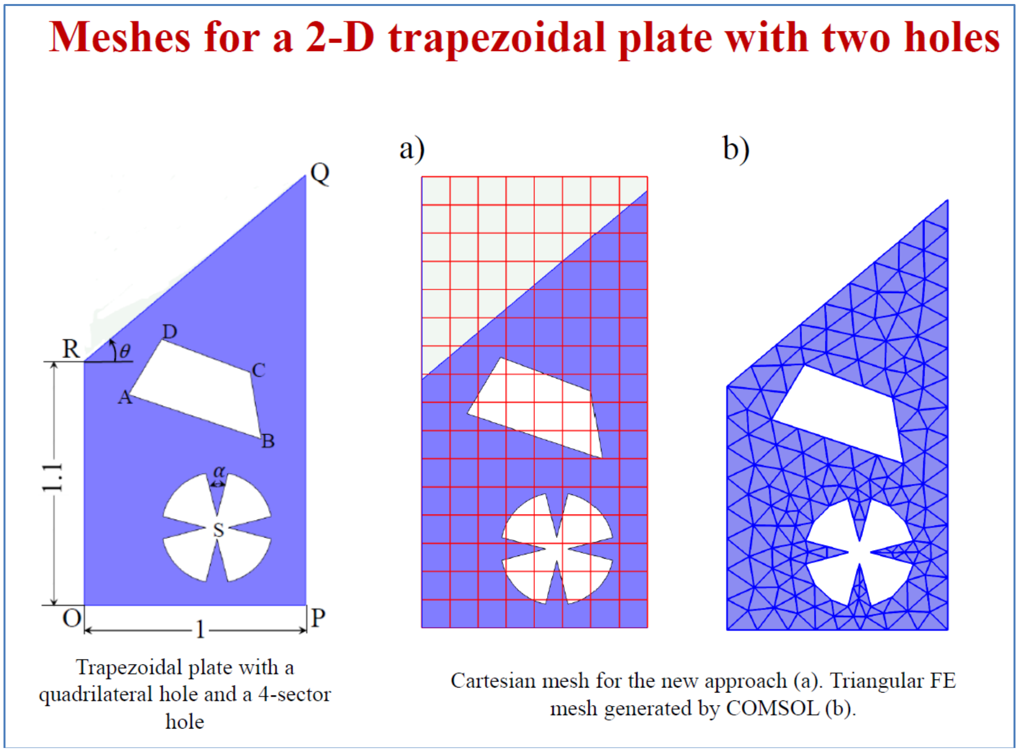

Fig.13. Highly oscillatory waves in a trapezoidal plate with two holes (Cartesian and FE meshes).

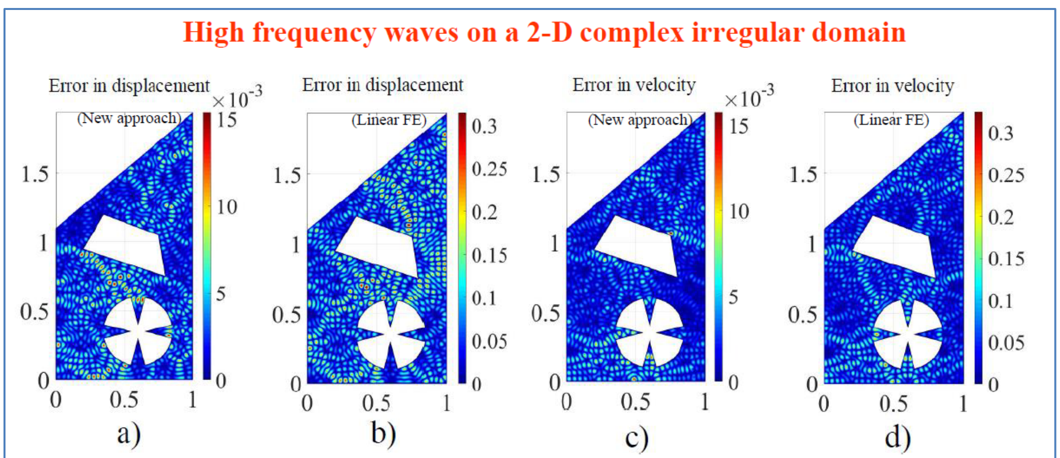

The error distributions in displacement (a, b) and in velocity (c, d) at the final time T=2 obtained by the new approach with 48,210 degrees of freedom (a, c) and by the linear triangular finite elements with 652,462 degrees of freedom (b, d)

Comparison of computational costs (the number of degrees of freedom) for the new approach and linear FEs

Maximum error	$NDoF_{New\ approach}$	$NDoF_{Linear\ FE}$	$\frac{NDoF_{Linear\ FE}}{NDoF_{New\ approach}}$
30%	11,263	652,462	58
15%	15,609	1,277,691	82
1.5%	48,210	13,000,000(estimated)	270

Fig.14. Highly oscillatory waves in a trapezoidal plate with two holes (the distribution of the error in displacement and velocity obtained by the new approach and the linear finite elements).

7.2. 3-D waves on an irregular domain with a hole.

Here we consider the application of the new approach with 27-point stencils (related to the computational costs of the linear finite elements) to wave propagation in a 3-D irregular domain represented by a trapezoidal prism with a spherical hole; see Fig. 15. Using the method of manufactured solutions, we select the exact solution presented in Fig. 16. The problem was solved by the new approach and by the conventional linear and high-order tetrahedral finite elements (typical meshes used by the new approach and by FEM are shown in Fig. 15). The comparison of the errors in displacement and velocity for these techniques is shown in Fig. 16 as a function of the number N of degrees of freedom at mesh refinement in the logarithmic scale. As can be seen from Fig. 16, at the same N the new approach yields much more accurate results than those obtained by the conventional linear and high-order (up to the seventh order) finite elements. It is important to mention that the higher order finite elements have much wider stencils and require a much more computation time compared to that for the new approach at the same N. It is also interesting to note that at accuracy of 5%, the new approach reduces the number of degrees of freedom by a factor of greater than 1000 compared to that for the linear finite elements with similar stencils (e.g., compare curves 1 and 8 in Fig. 16 at $\text{Log}_{10}\, e^{max}_{u} = -1.3$). This leads to a huge reduction in the computation time for the new approach at a given accuracy. This reduction in the computation time will be even greater if a higher accuracy is needed; e.g., 1% or less; see our paper [1] for more details.

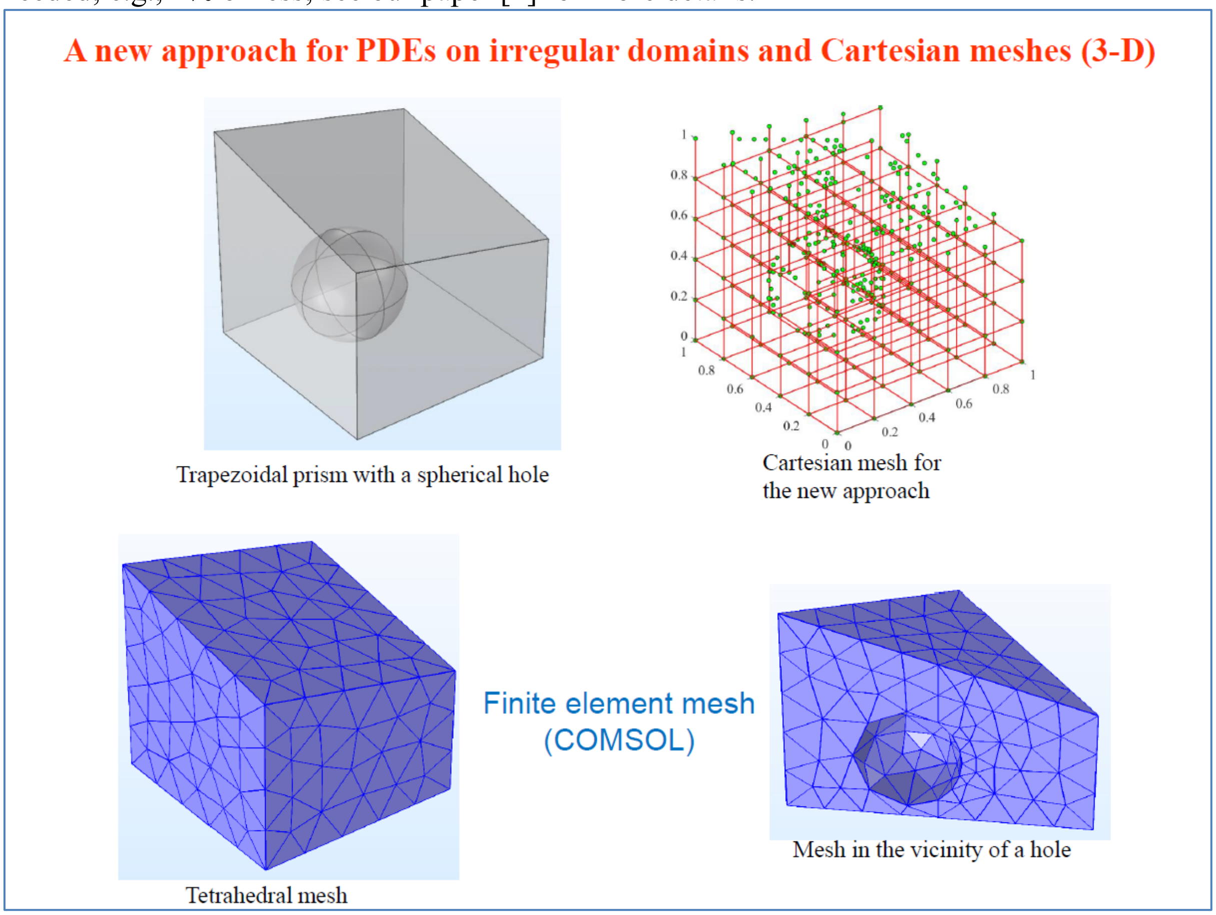

Fig.15. Wave propagation in a 3-D trapezoidal plate with a spherical holes (Cartesian and FE meshes).

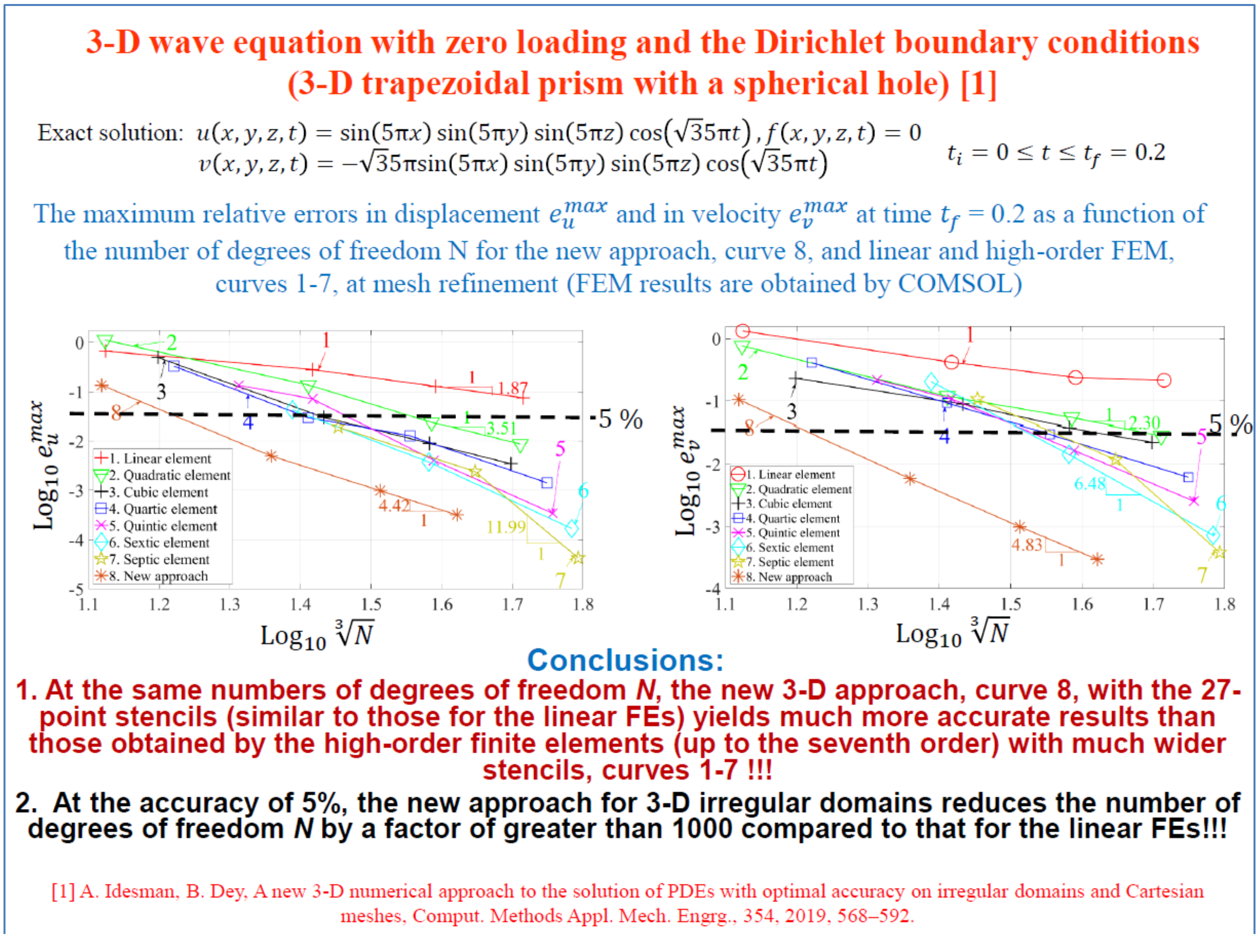

Fig.16. Wave propagation in a 3-D trapezoidal plate with a spherical hole (the error in displacement and velocity obtained by the new approach and by the linear and high-order finite elements).

7.3. 2-D waves in anisotropic functionally graded materials (an irregular domain)

In contrast to wave propagation problems in isotropic materials with constant material properties considered in the previous sections, here we show the application of the new approach to wave propagation in anisotropic functionally graded materials. In this case the material properties are different for different directions as well as they depend on the spatial coordinates. We consider the wave propagation in a trapezoidal plate with quadrilateral and spherical holes; see Fig. 17. Using the method of manufactured solutions, we select an exact solution with the different wave velocities c_x and c_y which are also the functions of the special coordinates, see Fig. 17. The problem was solved by the new approach with the 9-point stencils and by the conventional linear and high-order quadrilateral and triangular finite elements. Fig. 17 shows the distribution of the relative errors in velocity of the numerical solutions as well as the maximum error in velocity as a function of the number N of degrees of freedom for these two techniques. As can be seen from Fig. 17, at the same N the new approach yields much more accurate results than those obtained by the conventional linear and high-order (up to the third order) finite elements. It is important to mention that the higher order finite elements have much wider stencils and require a much more computation time compared to that for the new approach at the same N. It is also interesting to note that at accuracy of 10%, the new approach reduces the number of degrees of freedom by a factor of greater than 80 compared to that for the linear finite elements with similar stencils (e.g., compare curves 1 with 2 and 5 in Fig. 17). This leads to a huge reduction in the computation time for the new approach at a given accuracy. This reduction in computation time will be even greater if a higher accuracy is needed; e.g., 1% or less.

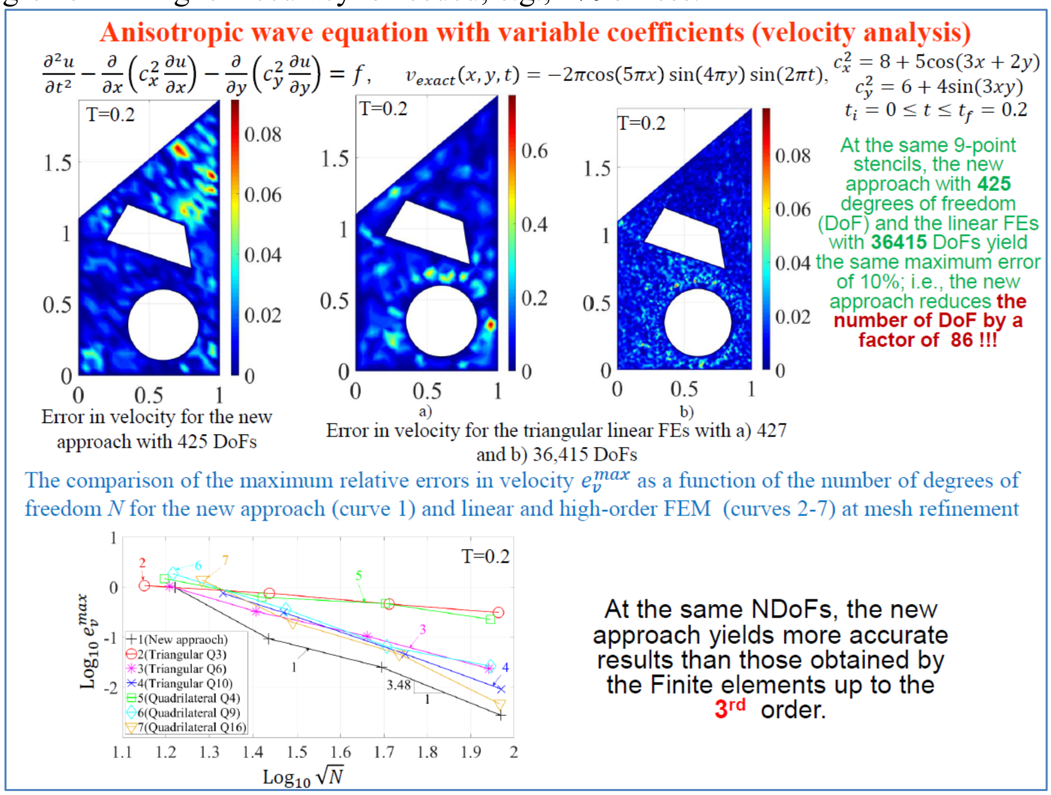

Fig.17. Wave propagation in anisotropic functionally graded materials (the distribution of the error in displacement and velocity obtained by the new approach and by the linear finite elements for a 2-D trapezoidal plate with two holes).

7.4. 1-D wave propagation impact problem

Here, we show that the new approach can be also applied to the problems with non-smooth solutions. Let use consider the 1-D impact problem for the wave equation with a propagating discontinuity for the velocity; see Figs. 18, 19. This problem with the discontinuous solution for the velocity is solved by the new approach and by the linear finite elements on the same meshes. It is known that the accurate time integration of the semidiscrete systems for impact problems may lead to large spurious oscillations in numerical results. Therefore, the two-stage time-integration procedure with the basic computations and the filtering stage (that has been developed in our papers) is used to obtain accurate and non-oscillatory numerical results. The basic calculations in this procedure correspond to the accurate time integration of the semidiscrete system. The velocity distributions along the bar after the stage of basic computations and after the filtering stage are shown in Fig. 18 for the new approach with matched meshes and for the linear finite elements on the same meshes. As can be seen, two considered approaches yield large spurious oscillation after basic computations. However, it is very easy to compare the numerical results after the filtering stage. As can be seen from Figs. 18 and 19, after the filtering stage the new approach yields more accurate results compared with the linear finite elements and these results are practically the same on matched (Fig. 18) and non-matched (Fig. 19) meshes; see also our paper [11] for more details.

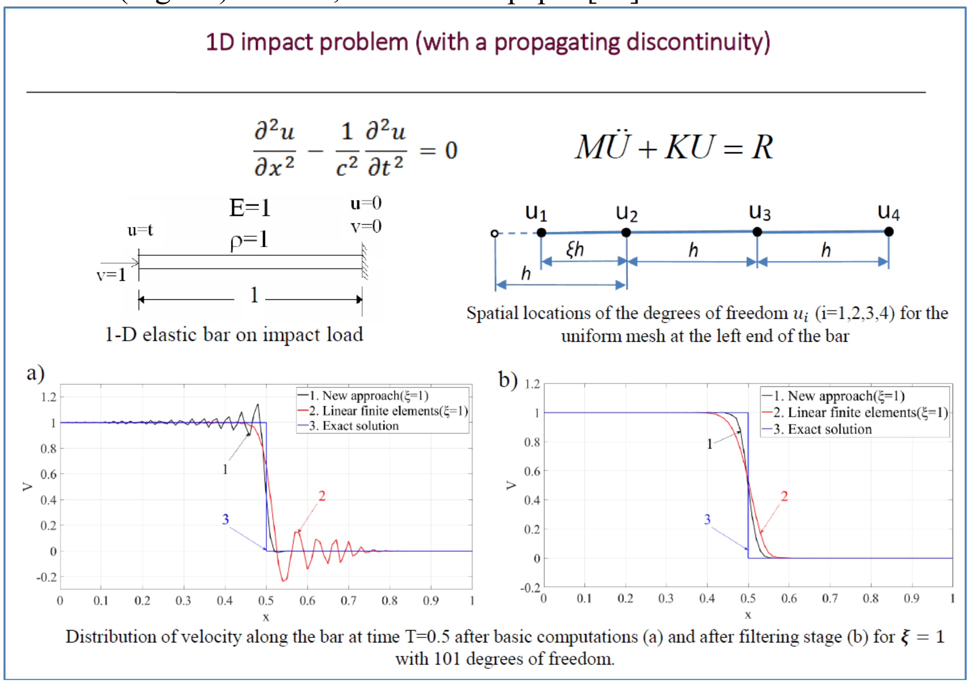

Fig.18. The 1-D impact problem with the propagating discontinuity for the velocity solved by the new approach and by the linear finite elements on matched meshes.

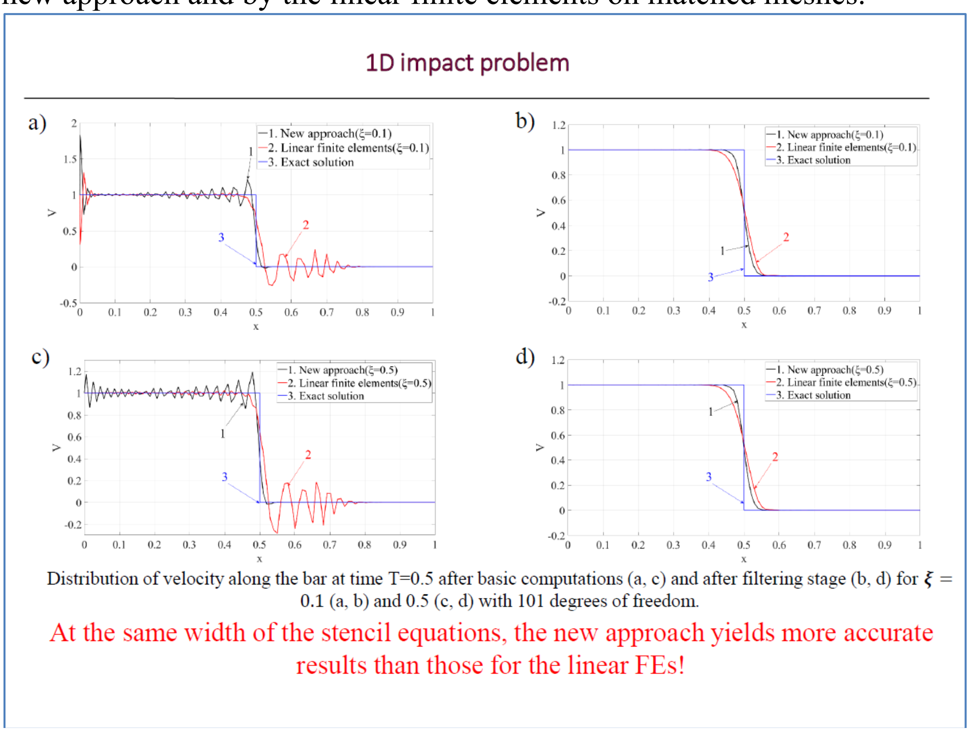

Fig.19. The 1-D impact problem with the propagating discontinuity for the velocity solved by the new approach and by the linear finite elements on nonmatched meshes.

7.5. A plate with a crack under impact loading.

Here we consider the application of the new approach to very important engineering problems related to the calculation of the dynamics stress intensity factors (DSIFs) for cracked bodies. An impact loading is applied to a plate with a crack that causes the propagation of elastic waves within the plate. Similar to the previous problem in section 7.4, we use the two-stage time integration technique with the basic computations and the filtering stage in order to remove spurious numerical high frequency oscillations under impact loading; see curve 1 in Fig. 20. The numerical results for the dynamics stress intensity factors in Fig. 21 show that on comparable meshes the new approach yields much more accurate numerical results compared to those obtained by the very popular XFEM which uses the special crack tip enrichment functions for the treatment of a singularity in the vicinity of the crack tip. This means that for an accurate solution of wave propagation problems with cracks, the accurate numerical solutions of general wave propagation problems are much more important than the use of the special crack tip enrichment functions; see also our paper [7] for more details.

.

Dynamic Stress Intensity Factors (DSIFs) for stationary mixed mode semi-infinite crack

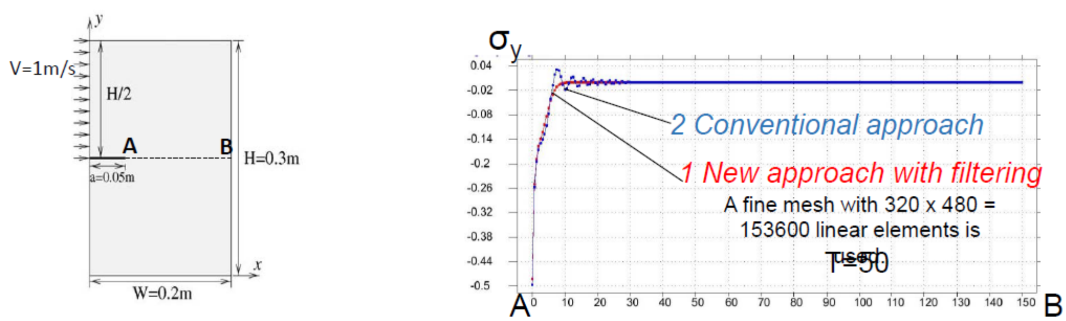

Figure. Geometry of a edge cracked semi-infinite plate under impact loading (a). The distribution of the σ_y stress in the vicinity of the crack tip along line AB at the time T=50 (b). Curve 1 corresponds to the numerical results with the linear elements with reduced dispersion after the filtering stage. Curve 2 corresponds to the numerical results with the conventional finite elements without the filtering stage.

Fig.20. A plate with a mixed-mode crack (geometry and the distribution of the σ_y stress along line AB)

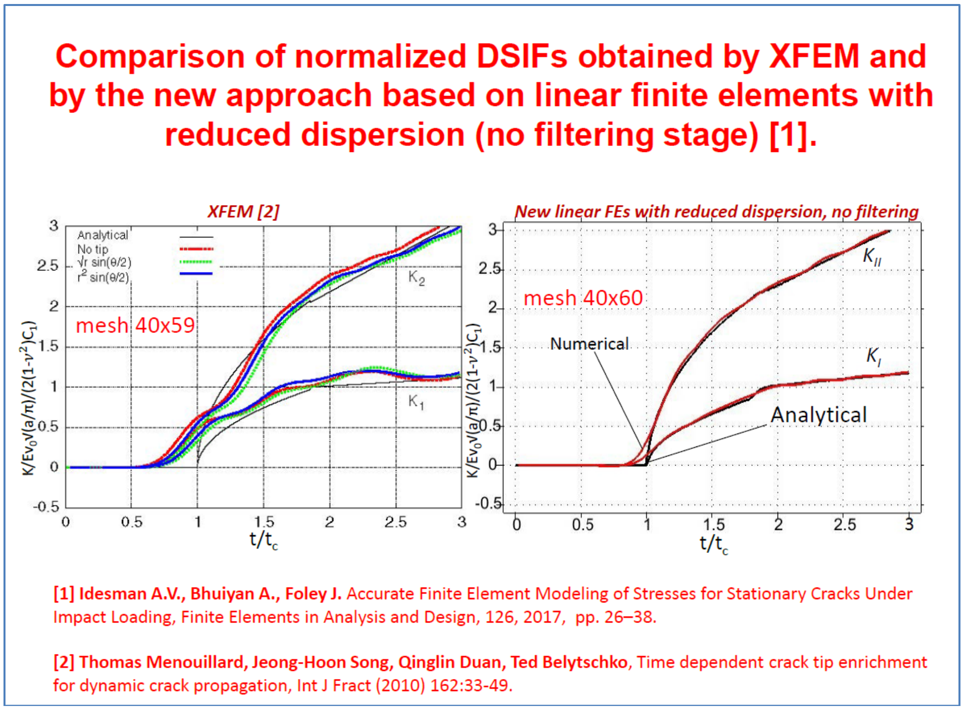

Fig.21. A plate with a mixed-mode crack (the dynamics stress intensity factors (DSIFs) obtained by the new approach and by XFEM).

8. Concluding remarks

Below Fig. 22 summarizes the main features and advantages of the new approach.

A new approach with optimal accuracy (based on the minimization of the local truncation error) for the wave and heat equations on irregular domains with Cartesian meshes

The main features and advantages of the new approach

1. The new approach does not use any weak formulation for the derivation of discrete equations. The coefficients in the discrete system are directly derived by the minimization of the order of the local truncation error and provide the optimal order of accuracy at a given width of stencil equations.
2. At the same computation costs (the same width of stencil equations), the new approach yields much higher order of accuracy than other numerical techniques (FEM, FD, FV, ISA and other). For example, at the similar 9-point 2-D stencils, the accuracy of the new approach is two orders higher than that for the linear finite elements. The new approach is even much more accurate than the high-order finite elements with much wider stencils. This also means that at a given accuracy, the new approach significantly reduces the computation time compared to known numerical techniques.
3. In contrast to the finite elements, spectral elements, isogeometric elements and other similar techniques used for irregular domains, the new approach uses trivial Cartesian meshes that requires practically negligible computation time for their preparation.
4. In contrast to the finite element techniques, a large difference in distances between neighboring grid points used in the same stencil does not lead to the degradation of accuracy. This is very important advantage of the new approach on irregular domains.
5. The new approach does not require time consuming numerical integration for finding the coefficients of the stencil equations; e.g., as for the high-order finite, spectral and isogeometric elements. For the new technique, the coefficients of the stencil equations for the grid points located far from the boundary are calculated analytically. For the grid points located close to the boundary (with non-uniform and cut stencils), the coefficients of the stencil equations are calculated numerically by the solution of very small local systems of linear algebraic equations.

Fig.22. The main features and advantages of the new approach.

9. Activities supported by the grant

Students

Two PhD students (one of them graduated in June 2018).

Publications

1. A new 3-D numerical approach to the solution of PDEs with optimal accuracy on irregular domains and Cartesian meshes. Idesman, A., Dey, B. Computer Methods in Applied Mechanics and Engineering, 2019, 354, pp. 568-592.
2. A new numerical approach to the solution of partial differential equations with optimal accuracy on irregular domains and Cartesian meshes., Idesman A.V. Proceedings of the 7th ECCOMAS Thematic Conference on Computational Methods in Structural Dynamics and Earthquake Engineering, Crete, Greece, 24-26 June, 2019, pp. 1-30.
3. The use of the local truncation error to improve arbitrary-order finite elements for the linear wave and heat equations., Idesman A.V. Computer Methods in Applied Mechanics and Engineering, 2018,334, pp. 268-312.
4. Optimal Reduction of Numerical Dispersion for Wave Propagation Problems. Part 2: Application to 2-D Isogeometric Elements, Idesman A.V., Dey B. Computer Methods in Applied Mechanics and Engineering, 2017, 321, pp. 235-268.
5. Optimal Reduction of Numerical Dispersion for Wave Propagation Problems. Part 1: Application to 1-D Isogeometric Elements., Idesman A.V. Computer Methods in Applied Mechanics and Engineering, 2017,317, pp. 970-992.
6. The use of the local truncation error for the increase in accuracy of the linear finite elements for heat transfer problems, Idesman A.V., Dey B. Computer Methods in Applied Mechanics and Engineering, 2017, 319, pp. 52-82.
7. Accurate Finite Element Simulation of Stresses for Stationary Dynamic Cracks under Impact Loading, Idesman A.V., Bhuiyan A., and Foley J. R. Finite Elements in Analysis and Design, 2017, 126, pp. 26-38 (the paper was one of the most downloaded Finite Elements in Analysis and Design articles within 90 days after publication).
8. Optimal reduction of numerical dispersion for wave propagation problems. Application to isogeometric elements., Idesman A.V. Proceedings of the 6th ECCOMAS Thematic Conference on Computational Methods in Structural Dynamics and Earthquake Engineering, Rhodes Island, Greece, 15-17 June, 2017, pp. 1-9.
9. Idesman A.V., Dey B., The use of the local truncation error for the increase in accuracy of high-order elements for heat transfer problems. Application to quadratic isogeometric elements., International Journal for Numerical Methods in Engineering, 2019, pp. 1-41 (under review).
10. Idesman A.V., A new numerical approach to the solution of partial differential equations with optimal accuracy on irregular domains and Cartesian meshes. Part 1: the derivations for the wave, heat and Laplace equations in the 1-D and 2-D cases., Applied Mathematical Modelling, 2019, pp. 1-31 (under review).
11. Dey B., Idesman A.V., A new numerical approach to the solution of partial differential equations with optimal accuracy on irregular domains and Cartesian meshes. Part 2:

numerical simulation and comparison with FEM., Applied Mathematical Modelling, 2019, pp. 1-33 (under review).

12. Idesman A.V., Dey B., The treatment of the Neumann boundary conditions for a new numerical approach to the solution of PDEs with optimal accuracy on irregular domains and Cartesian meshes., Computer Methods in Applied Mechanics and Engineering, 2019, pp. 1-29 (under review).
13. Idesman A.V., Dey B., Accurate numerical solutions of 2-D elastodynamics problems using compact high-order stencils., Computer and Structures, 2019, pp. 1-26 (under review).
14. Idesman A.V., Dey B., Compact high-order stencils with optimal accuracy for numerical solutions of 2-D time-independent elasticity equations., Computer Methods in Applied Mechanics and Engineering, 2019, pp. 1-19 (under review).

Presentations

- ***Six Keynote lectures:*** *at the 6th ECCOMAS Thematic Conference on Computational Structural Dynamics and Earthquake Engineering, Rhodes Island, Greece (June 15, 2017), at the 14th U.S. National Congress on Computational Mechanics, Montreal, Canada (July 17, 2017), at the 13th World Congress on Computational Mechanics (WCCM 2018), New York, USA (July 25, 2018), at the 6th European Conference on Computational Mechanics (Solids, Structures and Coupled Problems) (ECCM 6) and the 7th European Conference on Computational Fluid Dynamics (ECFD 7) jointly organized in Glasgow, UK (June 14, 2018), at the 7th ECCOMAS Thematic Conference on Computational Structural Dynamics and Earthquake Engineering, Crete, Greece (June 24, 2019), at the 15th U.S. National Congress on Computational Mechanics, Austin, USA (July 30, 2019)*

- ***Three Invited lectures:*** **the seminar at the Air Force Institute of Technology**, Dayton, OH, USA, April 12, 2018, **the seminar of the Universität Duisburg-Essen**, Essen, Germany, July 10, 2017, **the seminar at Sandia**, Albuquerque, NM, USA, March 13, 2017.

- **Organizer of six mini-symposia at:** the 14th and 15th U.S. National Congress on Computational Mechanics (July 2017), (July 2019), the 6th and 7th ECCOMAS Thematic Conference on Computational Structural Dynamics and Earthquake Engineering, Greece (June, 2017), (June, 2019), the 13th World Congress on Computational Mechanics (WCCM 2018), New York, USA (July, 2018), the 6th European Conference on Computational Mechanics (Solids, Structures and Coupled Problems) (ECCM 6) and the 7th European Conference on Computational Fluid Dynamics (ECFD 7) jointly organized in Glasgow, UK (June, 2018)